British Journal of Pharmacology

DOI:10.1111/bph.12351
www.brjpharmacol.org

RESEARCH PAPER

The serine-threonine kinase p90RSK is a new target of enzastaurin in follicular lymphoma cells

S Kheirallah[1–5], S Fruchon[6], L Ysebaert[1–5,7], A Blanc[1–5], F Capilla[8], A Marrot[8], T AlSaati[8], F X Frenois[9], K A Benhadji[10], J J Fournié[1–5], G Laurent[1–5,7] and C Bezombes[1–5]

[1]*INSERM UMR1037-Centre de Recherche en Cancérologie de Toulouse, Toulouse, France,* [2]*Université Toulouse III Paul-Sabatier, Toulouse, France,* [3]*ERL 5294 CNRS, BP3028, Hôpital Purpan, Toulouse, France,* [4]*Institut Carnot Lymphome-CALYM, Toulouse, France,* [5]*Laboratoire d'Excellence Toulouse Cancer-TOUCAN, Toulouse, France,* [6]*INSERM UMR1043-Centre de Physiopathologie Toulouse Purpan, Toulouse, France,* [7]*Service d'Hématologie, CHU Purpan, Toulouse, France,* [8]*INSERM, US006, ANEXPLO/CREFRE, Service d'Histopathologie, Hôpital Purpan, Toulouse, France,* [9]*Service Anatomie Pathologique CHU Toulouse, Hôpital Purpan, Toulouse, France, and* [10]*Lilly Corporate Center, Eli Lilly. Suresnes, France*

Correspondence
Dr Christine Bezombes, INSERM U1037 – CRCT, CHU Purpan – BP3028, Toulouse 31300, France. E-mail: christine.bezombes-cagnac@inserm.fr

Keywords
apoptosis; enzastaurin; follicular lymphoma; Bad; GSK3β; p90RSK

Received
5 November 2012
Revised
23 May 2013
Accepted
7 June 2013

BACKGROUND AND PURPOSE

Follicular lymphoma is the second most common non-Hodgkin's lymphoma and, despite the introduction of rituximab for its treatment, this disease is still considered incurable. Besides genetic alterations involving Bcl-2, Bcl-6 or c-Myc, follicular lymphoma cells often display altered B-cell receptor signalling pathways including overactive PKC and PI3K/Akt systems.

EXPERIMENTAL APPROACH

The effect of enzastaurin, an inhibitor of PKC, was evaluated both *in vitro* on follicular lymphoma cell lines and *in vivo* on a xenograft murine model. Using pharmacological inhibitors and siRNA transfection, we determined the different signalling pathways after enzastaurin treatment.

KEY RESULTS

Enzastaurin inhibited the serine-threonine kinase p90RSK which has downstream effects on GSK3β. Bad and p70S6K. These signalling proteins control follicular lymphoma cell survival and apoptosis; which accounted for the inhibition by enzastaurin of cell survival and its induction of apoptosis of follicular lymphoma cell lines *in vitro.* Importantly, these results were replicated *in vivo* where enzastaurin inhibited the growth of follicular lymphoma xenografts in mice.

CONCLUSIONS AND IMPLICATIONS

The targeting of p90RSK by enzastaurin represents a new therapeutic option for the treatment of follicular lymphoma.

Abbreviations

FL, follicular lymphoma; DLBCL, diffuse large B-cell lymphoma; BCR, B-cell receptor; p70S6K, p70S6 kinase

Introduction

The current combination regimen for treating follicular lymphoma (FL) combines chemotherapy with immunotherapy through the use of monoclonal antibodies. Despite this, most patients relapse sooner or later, so there is still need for new therapeutic targets. The molecular basis of FL relies upon accumulation of genetic alterations such as the

t(14;18) translocation which causes overexpression of the anti-apoptotic protein Bcl-2 and is found in 85% of FL cases. However, Bcl-2 transgenic mice do not develop FL spontaneously and FL patients that do not carry the t(14;18) translocation have the same clinical outcome (Alexander *et al.*, 2007). This suggests that this genetic abnormality alone is insufficient to cause the disease and induce post-therapeutic relapses.

Other alterations of signalling pathways have recently been characterized in FL cells. B-Cell receptor (BCR signalling is activated in tumour cells from FL patients (Irish *et al.*, 2006) and these cells also overexpress a phosphorylated (active) form of the pro-survival protein Akt (Zha *et al.*, 2004; Gulmann *et al.*, 2005). We found that Syk-mediated activation of mTOR was critical in determining the survival and clonogenic potential of FL cells (Leseux *et al.*, 2006). Other kinases can also contribute to mTOR deregulation in FL cells, for example overactivation of PI3K/Akt, PKCζ and PLD also lead to phosphorylation of constitutive p70S6 kinase (p70S6K) on Thr^{389}, thereby activating mTOR (Leseux *et al.*, 2006; 2008). mTOR is regulated by many kinases including PKC (Guertin and Sabatini, 2007). PKC is known to play a role in lymphomagenesis (Leitges *et al.*, 1996) and its isoform PKCβ is overexpressed in FL and diffuse large B-cell lymphoma (DLBCL) (Shipp *et al.*, 2002; Hans *et al.*, 2005; Decouvelaere *et al.*, 2007). PKCβ plays an important role in B-cell signalling and survival and, accordingly, PKCβ-deficient mice exhibit strongly impaired B-cell functions (Leitges *et al.*, 1996). The acyclic bisindolylmaleimide enzastaurin is a PKCβ inhibitor which displays anti-tumour activity towards various cancers (Chen and LaCasce, 2008; Ysebaert and Morschhauser, 2011). Civallero *et al*. reported that enzastaurin induced apoptosis in FL cells and inhibited Akt, another ribosomal kinase p90RSK and GSK3 (Civallero *et al.*, 2010).

We surmised that enzastaurin could be a useful tool for investigating the hierarchy of connections between these signalling pathways in FL cells, thus improving our understanding of the intracellular mechanisms of FL oncogenesis to help identify new pharmacological targets. We report here that p90RSK controls both the mTOR-mediated pro-survival pathway and the Bad-mediated pro-apoptotic pathway. Hence, by inhibiting p90RSK in FL cells, enzastaurin simultaneously blocks pro-survival signalling and activates the apoptotic cascade. Importantly, these effects translate to an anti-tumour pharmacological activity against FL cells both *in vitro* and *in vivo*, validating p90RSK as a new target for FL treatment.

Methods

Cell lines

RL, DOHH2 and Karpas-422 are transformed FL cell lines carrying the t(14;18) translocation. RL and DOHH2 were obtained from the ATCC (Rockville, MD, USA), Karpas-422 from the DSMZ cell collection (Braunschweig, Germany). Cells were cultured at 37°C in 5 % CO_2 in RPMI supplemented with 10 % fetal calf serum (FCS), glutamine (2 mM), streptomycin (10 μg ml^{-1}) and penicillin (200 U ml^{-1}) (Invitrogen, Cergy Pontoise, France).

Cell viability

FL cell lines were seeded at 4 x 10^5 cells mL^{-1} and were treated with various concentrations of enzastaurin. Cell viability was evaluated after 24 and 48 h by counting cells using the Trypan blue exclusion method.

Cell cycle analysis and DAPI staining

After washing in PBS, FL cells were permeabilized in a PBS solution containing 0.1 % Triton X-100 and 1 μg mL^{-1} RNaseA for 1 min. After 2 min of centrifugation, pellets were resuspended for 15 min in PBS containing DAPI at 10 μg mL^{-1} and cell cycle progression was analysed using a BDLSRII cytometer (Becton Dickinson, Le Pont de Claix, France) and DIVA 6.1.2 software. For DNA staining visualization, a Nikon Eclipse TE2000-U fluorescent microscope (Champigny sur Marne, France) was used.

Western blotting

Analyses were performed as previously described (Leseux *et al.*, 2006). Antibodies were all purchased from Ozyme (St Quentin en Yvelines, France) and used according to the manufacturer's recommendations. HRP–conjugated secondary antibodies against rabbit, mouse or goat immunoglobulins were from Beckman Coulter (Marseille, France).

siRNA *transfection*

RL cells were transfected using Amaxa nucleofector kit V (Lonza, Levallois-Perret, France). Five million cells were transfected twice (24 h between each) with 950 nM p90RSK siRNA or scrambled siRNA as a control (Dharmacon, Brebières, France). Four hours after transfection, cells were seeded at 3 × 10^5 cells mL^{-1} in RPMI 10% FCS. Protein depletion was assessed 48 h after the second transfection via Western blot analysis.

FL xenograft murine model

All animal care and experimental procedures were approved by the INSERM Animal Care and Use Committee. All studies involving animals are reported in accordance with the ARRIVE guidelines for reporting experiments involving animals (Kilkenny *et al.*, 2010; McGrath *et al.*, 2010). A total of 20 animals were used in the experiments described here. RL cells (10^7) resuspended in 300 μl PBS, were subcutaneously injected into the right flank of SCID-Beige mice. When tumour volumes reached 100 mm^3, mice were divided into two groups of eight to 10 animals. One group was treated by oral gavage once daily with 150 mg kg^{-1} of Enzastaurin dissolved in a 10% acacia gum solution (Fisher Scientific, Ilkirch, France) containing 1/6 Intralipid (Sigma Aldrich, St Quentin Fallavier, France) and 0.5% Tween 80 (VWR, Fontenay-sous-Bois, France). The control group was treated with the vehicle following the same schedule and route of administration. Tumour burden was measured three times per week with a caliper, and tumour volume (TV) was calculated using the formula TV = (length × $width^2$)/2. Animals were killed when the TV reached 1600–1800 mm^3.

Caspase 3 and phospho-p90RSK immunostaining

Caspase 3 and phospho-p90RSK immunostaining was carried out as previously described (Fruchon *et al.*, 2012) on xenograft FL tumours (10 animals for each condition of treatment) using specific antibodies (R&D systems, Lille, France).

In vivo *caspase 3 and phospho-p90RSK positive cell quantification*

Immunohistochemical-stained slides were digitized in brightfield scan mode using the Panoramic 250 Flash digital microscope (3DHISTECH, Budapest, Hungary) equipped with a 20X/NA 0.80 Zeiss Plan-Apochromat dry objective and a 2 megapixel 3CCD colour camera (CIS Americas Inc., Tokyo, Japan), and allowing a resolution of 0.22 µm/pixel (corresponds to a 56.09 × magnification at the highest optical resolution).

The Panoramic Viewer (RTM 1.15.0.53) and the additional HistoQuant module (RTM 1.15.0.53) were used for viewing and analysing the digital slides respectively (3DHISTECH). A minimum of five annotations per slide covering more than 80% of the entire tissue were analysed. Automatic segmentation of the detected objects and measurement of the number of detected objects per mm^2 were carried out.

Data analysis

For the histogram analyses, data shown represent means ± SD. Means were compared using unpaired, two-tailed Student's *t*-tests, and $p < 0.05$ was considered statistically significant.

Materials

DMSO, ZVAD-*Fmk* and wortmannin were purchased from Sigma Aldrich (St Quentin Fallavier, France). Enzastaurin was kindly provided by Eli Lilly (Suresnes, France).

Results

Enzastaurin inhibits classical targets in FL cells

Enzastaurin is known to induce an anti-proliferative effect in many tumour cells *via* the PI3K/Akt pathway (Chen and LaCasce, 2008; Ysebaert and Morschhauser, 2011). Studies have indicated that Akt inhibition occurs 48–72 h after treatment because two of its targets, GSK3β and p70S6K, are dephosphorylated at this time (Civallero *et al.*, 2010). We therefore analysed the activity levels of GSK3β, the PI3K/Akt module, and p70S6K in FL cells following enzastaurin treatment. In the three FL cell lines used, enzastaurin induced a huge decrease in GSK3β phosphorylation on its Ser^9 inhibitory site after only 6 h of treatment (Figure 1A). At the same

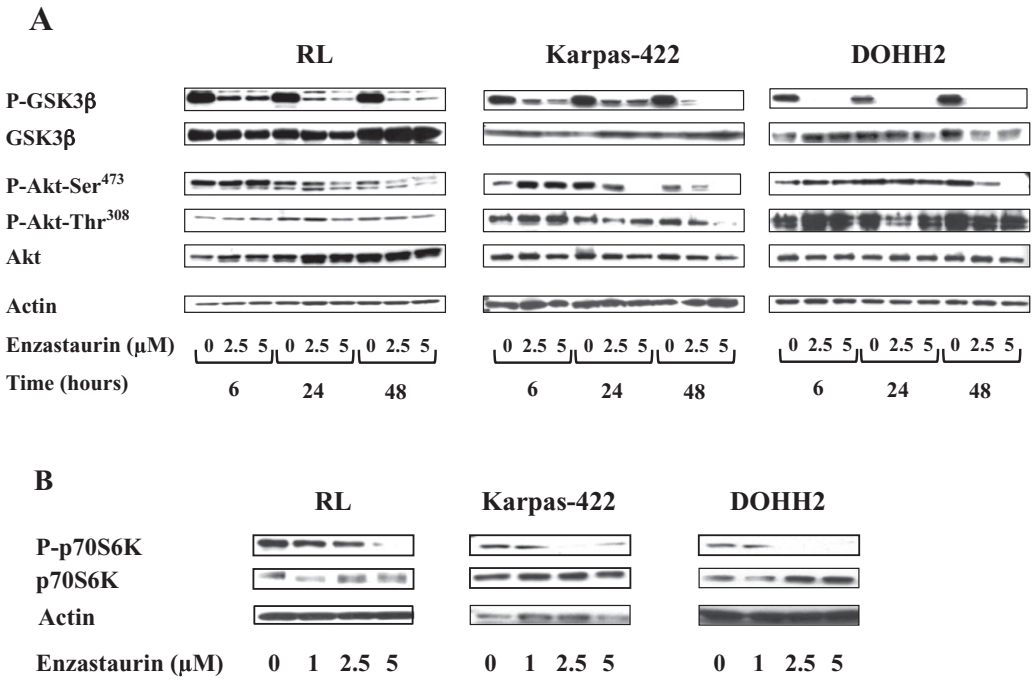

Figure 1

Inhibition of classical targets of enzastaurin in FL cells. (A) RL, Karpas-422 and DOHH2 cells were treated with a range of concentrations of enzastaurin or DMSO as control and the phosphorylation of GSK3β and Akt was determined at different times by Western blot analysis using specific anti-phospho-protein antibodies. GSK3β, Akt and actin expression were used as controls for protein expression. (B) RL, Karpas-422 and DOHH2 cells were treated with a range of concentrations of enzastaurin for 6 h or DMSO as control. mTOR activity was determined by Western blot analysis using an anti-phospho-p70S6K antibody. p70S6K and actin expression were used as controls for protein expression. All results presented are representative of three independent experiments.

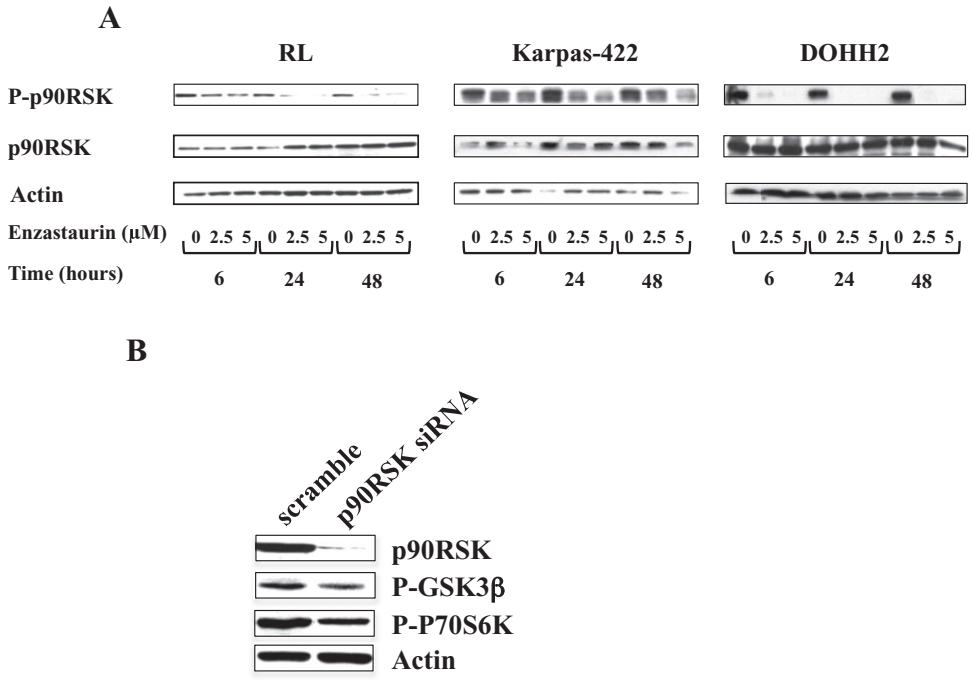

Figure 2

Inhibition of p90RSK and subsequent targets by Enzastaurin in FL cells. (A) RL, Karpas-422 and DOHH2 cells were treated with the indicated concentrations of enzastaurin for 6, 24 or 48 h or DMSO as control. The status of p90RSK phosphorylation was determined by Western blot analysis using a specific anti-phospho-protein antibody. p90RSK and actin expression were used as a control of protein expression. (B) RL cells were transfected by p90RSK siRNA and phosphorylation of p70S6K and GSK3β was evaluated by Western blot analysis. Actin expression was used as a control of protein expression. All results presented are representative of three independent experiments.

time point, no inhibition of Akt phosphorylation was observed at the Thr^{308} or Ser^{473} sites (Figure 1A), and no effects on PI3K activity (data not shown) were detected; these phenomena occurred later (24 and 48 h respectively). Within 6 h, enzastaurin also induced a rapid decrease in mTOR activity, as attested by the inhibition of the phosphorylated form of its target, p70S6K (Figure 2A).

These results demonstrate that, in FL cell lines, enzastaurin altered cellular signalling pathways, as illustrated by GSK3β-Ser^{9} dephosphorylation, and inhibited mTOR independently of the classically described Akt pathway.

p90RSK mediates enzastaurin-induced effects on GSK3β and p70S6K

To understand how enzastaurin exerts its rapid action on GSK3β and mTOR independently of Akt, we speculated that enzastaurin could inhibit p90RSK, which phosphorylates GSK3β on Ser^{9} and indirectly activates mTOR by inhibiting its repressor TSC2 (Anjum and Blenis, 2008). Thus, we evaluated the effect of p90RSK depletion with siRNA, on the GSK3β and mTOR phosphorylation status, induced by enzastaurin. As shown in Figure 2A, enzastaurin inhibited p90RSK phosphorylation (Thr^{359}/Ser^{363}) within 6 h. This shows that p90RSK is targeted by enzastaurin in the same time-frame as the dephosphorylation of its two targets, GSK3β and mTOR. In order to check that p90RSK regulates GSK3β and mTOR in FL cells, RL cells transfected with p90RSK siRNA were tested for their response to enzastaurin. As shown in Figure 2B, p90RSK silencing strongly decreased GSK3β and p70S6K phosphorylation. Thus, p90RSK mediates the effects of enzastaurin on the mTOR survival pathway in FL cells. These results prompted us to investigate its role in apoptosis.

Enzastaurin induces apoptosis through inhibition of p90RSK-mediated phosphorylation of Bad

The unphosphorylated form of the pro-apoptotic protein Bad is associated with Bcl-2 or Bcl_{XL} and inhibits their anti-apoptotic functions. Upon phosphorylation by different kinases including p90RSK (on Ser^{112}) and Akt (on Ser^{136}), Bad is sequestered by the 14-3-3 protein. This releases Bcl-2 and Bcl_{XL} to inhibit apoptosis by preventing cytochrome c release and caspase activation (Danial, 2008). In FL cells, we observed that, after 6 h of treatment, enzastaurin decreased Bad phosphorylation levels on its p90RSK-dependent Ser^{112} site whereas dephosphorylation of the Akt-dependent Ser^{136} site did not occur until after 48 h of treatment, as a consequence of Akt inhibition (Figure 3A). The regulation of Bad-Ser^{112} phosphorylation by p90RSK was confirmed by p90RSK gene silencing (Figure 3B). Moreover, Bad Ser^{136} phosphorylation by Akt was confirmed using wortmannin, a PI3K inhibitor (Figure 3C).

These results show that enzastaurin modulated both survival (mTOR) and apoptotic (Bad) pathways through the rapid inhibition of p90RSK.

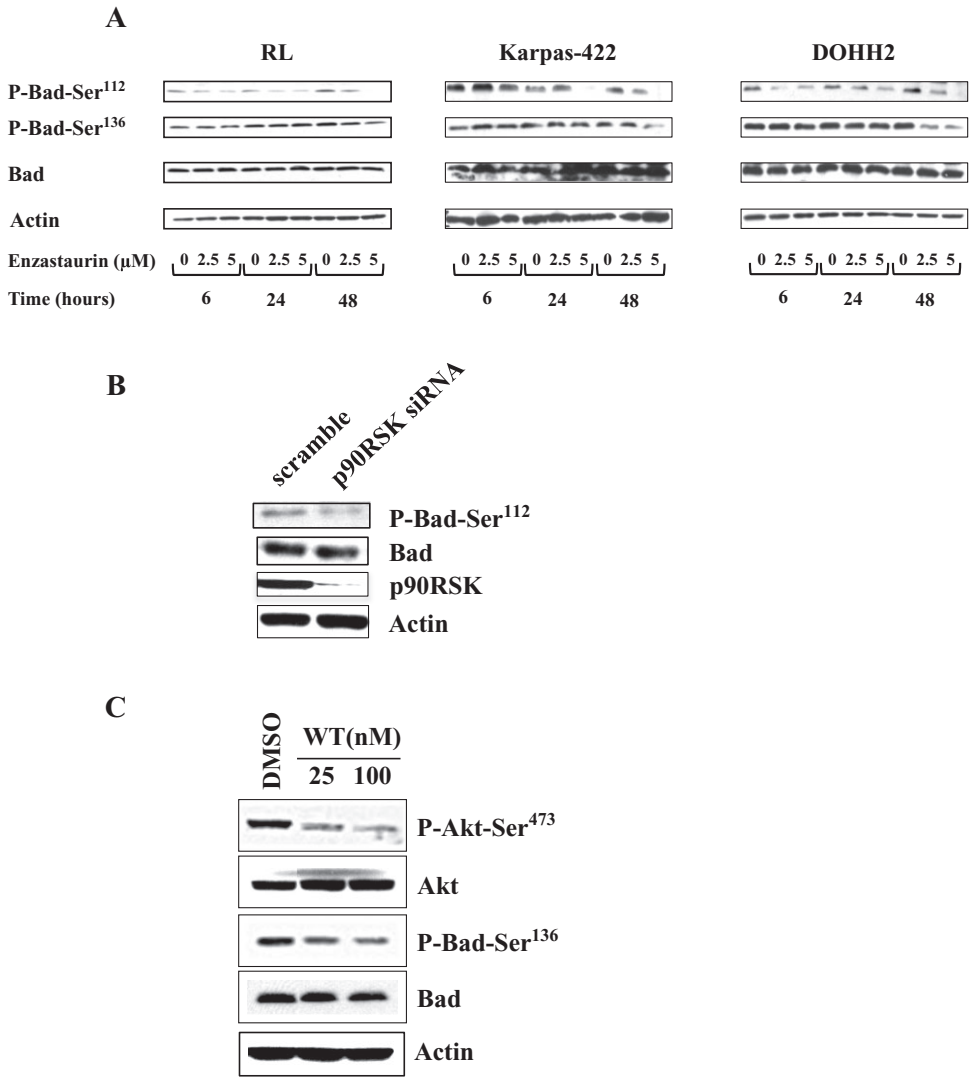

Figure 3

Inhibition of Bad phosphorylation. (A) RL, Karpas-422 and DOHH2 cells were treated with the indicated doses of enzastaurin for 6, 24 or 48 h or DMSO as control. Bad phosphorylation levels were determined by Western blot analysis using specific anti-phospho-protein antibodies. Bad and actin expression were used as a control of protein expression. (B) RL cells were transfected by p90RSK siRNA and Bad phosphorylation on Ser^{112} was evaluated by Western blot analysis. Bad and actin expression were used as a control of protein expression. (C) RL cells were treated for 1 h with wortmannin at 25 and 100 nM. Phosphorylation of Akt and Bad on Ser^{473} and Ser^{136}, respectively was determined using anti-phospho-protein antibodies. Akt, Bad and actin expression was used as a control of protein expression. All results presented are representative of three independent experiments.

Enzastaurin inhibits cell proliferation and induces apoptosis of FL cells in vitro

The cellular effects of enzastaurin were assessed on the FL cell lines RL, DOHH2 and Karpas-422. As shown in Figure 4A, enzastaurin caused a reduction of the number of viable FL cells when evaluated at 24 and 48 h post-treatment. We measured apoptosis by staining cells with DAPI followed by flow cytometry analysis. Enzastaurin induced apoptosis as revealed by an increased proportion of cells in sub-G1 phase (Figure 4B) and increased DNA fragmentation (Figure 4C). A role for caspases in the pro-apoptotic activity of enzastaurin was confirmed by pre-incubating RL cells with ZVAD-*fmk*, a pan-caspase inhibitor, which partly prevented the increase in the subG1 population (Figure 4B). Finally, we also confirmed that the enzastaurin-induced apoptosis involved caspase-3 and PARP cleavage (Figure 4D).

Together, these results demonstrate that, in FL cell lines, enzastaurin inhibits cell proliferation and activates apoptosis.

Enzastaurin is a potent anti-tumour agent in a FL xenograft model

Finally, we assessed the effects of enzastaurin in FL cells *in vivo,* as enzastaurin exhibits *in vivo* activity against various other cancers (Graff *et al.*, 2005; Moreau *et al.*, 2007; Podar *et al.*, 2007a). We injected RL cells subcutaneously into SCIB-Beige mice which received enzastaurin daily by oral gavage at

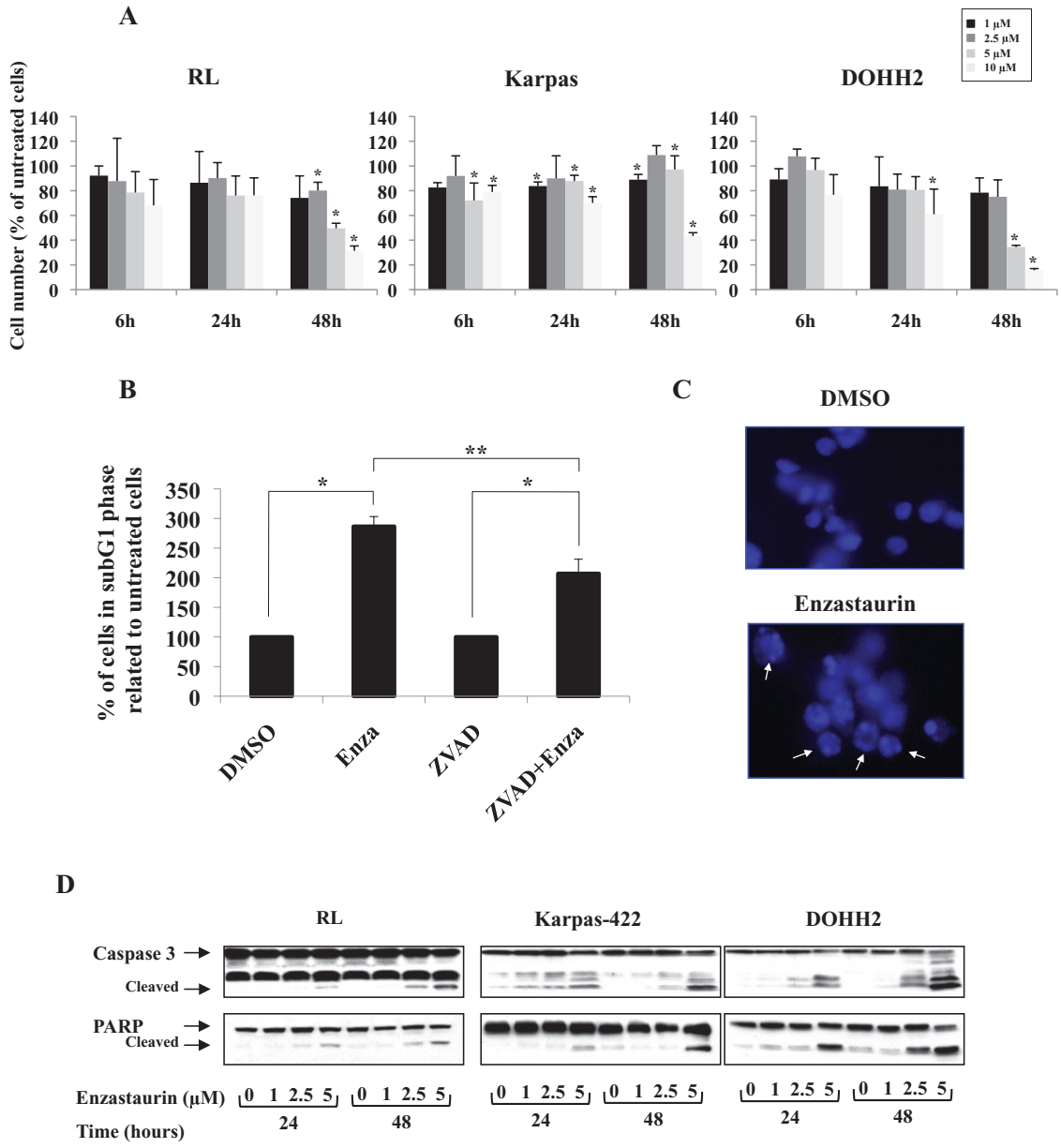

Figure 4

Biological effects of enzastaurin in FL cells. (A) RL, Karpas-422 and DOHH2 cells were treated with enzastaurin (1 to 10 µM) or DMSO as control and viable cells were determined by cell counting after 6, 24 and 48 h of treatment. Results are the mean of three independent experiments ± SD. *$P < 0.05$ compared to untreated cells. (B) RL cells were pre-incubated or not with 30 µM ZVAD-*Fmk* for 90 min then treated with 10 µM enzastaurin (Enza) for 48 h or DMSO as control. The percentage of cells in subG1 phase was determined by analysing the cell cycle. Histograms are expressed as a percentage of untreated cells and are the mean of three independent experiments ± SD. *$P < 0.05$ for enzastaurin-treated compared to DMSO-treated cells, and cells treated with ZVAD + enzastaurin compared to ZVAD alone. **$P < 0.05$ for cells treated with ZVAD + enzastaurin compared with enzastaurin alone. (C) RL cells were treated with 10 µM enzastaurin for 48 h and nuclear condensation was visualized under a fluorescent microscope after DAPI staining. (D) RL, Karpas-422 and DOHH2 cells were treated with various concentrations of enzastaurin or DMSO as control> Then caspase 3 and PARP cleavage were determined after 24 and 48 h of treatment, by Western blot analysis. Results are representative of three independent experiments.

150 mg kg^{-1}. Growth of tumour mass was monitored three times per week. As shown in Figure 5A, enzastaurin inhibited tumour growth, supporting the hypothesis that enzastaurin exhibits an anti-lymphomatous activity *in vivo*. This conclusion was supported by an increased immunostaining for active caspase 3, shown in xenografts isolated from enzastaurin-treated mice (Figure 5C and D), when compared to vehicle-treated animals (Figure 5B and D). Moreover, we determined *in vivo* the targeting of p90RSK by enzastaurin by analysing phospho-p90RSK (Thr^{359}/Ser^{363}) on tumours. As shown in Figure 6, enzastaurin induced a potent inhibition of p90RSK activity.

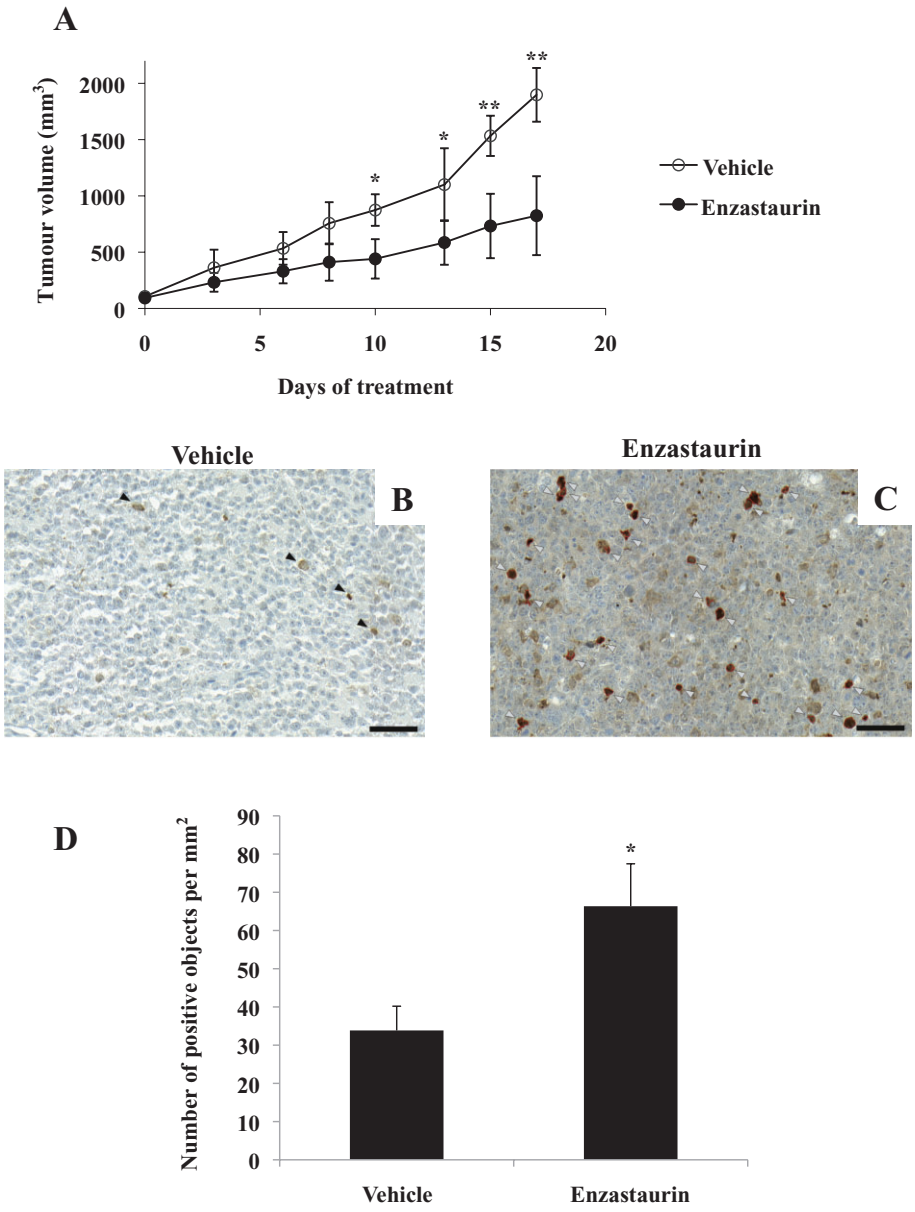

Figure 5

Anti-tumour effect and apoptosis induction by enzastaurin *in vivo*. (A) SCID-Beige mice engrafted with RL cells were treated with 150 mg kg^{-1} of enzastaurin, or vehicle, daily for 17 days. Results represent tumour volume calculated as described in the Methods, shown as means ± SD; **P* < 0.01; ***P* < 0.05 compared with enzastaurin-treated mice. (B, C) Photomicrographs acquired using the Panoramic Viewer software at the highest optical resolution (56.09×), illustrating the caspase 3 immunohistochemical staining (brown stained cells) in tumour tissue extracted from enzastaurin-treated animals (C), compared with vehicle-treated animals (B). Black arrowheads point to light stained cells in control animals. Grey arrowheads point to strongly stained cells in enzastaurin-treated animals. The red outlines superimposed on (C) show the automatic segmentation results using the .misp profile on this image (grey arrowheads). Scale bar = 50 μm. (D) Semi-quantitative data of caspase 3 immunopositive objects (cells) in enzastaurin-treated animals versus control animals. Histograms represent the mean ± SEM of the number of caspase 3 immunopositive objects per mm^2 (unpaired *t*-test: **P* = 0.0179 compared to the vehicle-treated group).

These results demonstrated that enzastaurin displayed *in vivo* anti-tumour effects in a FL xenograft model.

Discussion

BCR signalling molecules represent interesting targets in the development of new FL therapies. Our study provides *in vitro* and *in vivo* evidence supporting enzastaurin as a promising therapeutic molecule in the treatment of FL and highlights p90RSK as a key player in the cellular response to enzastaurin treatment. We established that, in FL cells, the p90RSK acts upstream of GSK3β, Bad and mTOR, and demonstrated a chronological cascade whereby p90RSK, mTOR and GSK3β modulation is followed by Akt inhibition. The fact that enzastaurin inhibited Akt on Thr^{308} and Ser^{473} suggests that both

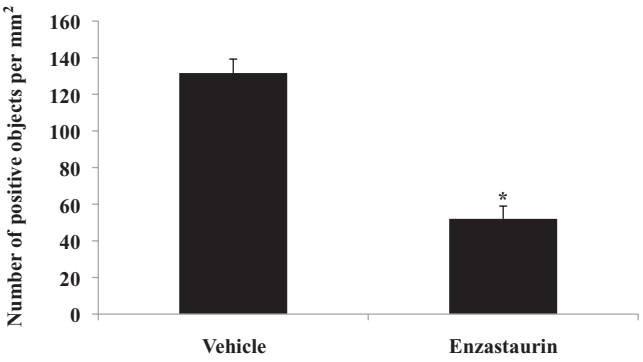

Figure 6

In vivo phospho-p90RSK targeting by enzastaurin. Semi-quantitative data of phospho-p90RSK immunopositive objects (cells) in enzastaurin-treated animals compared with control animals. Histograms represent the mean ± SEM of the number of phospho-p90RSK immunopositive objects per mm^2 ;unpaired t-test: *$P = 0.0179$ compared to the vehicle-treated group.

PI3K and mTOR are inhibited respectively. Moreover, we observed a decrease in Bad phosphorylation which induces its association with Bcl-2 or Bcl_{XL}, thereby inhibiting their anti-apoptotic functions. So despite the overexpression of Bcl-2 conferred by the t(14;18) translocation, enzastaurin can counteract this system and induce apoptosis to inhibit FL cell survival. This phenomenon is due, in part, to activation of caspases, because the pan-caspase inhibitor ZVAD did not completely inhibit enzastaurin-induced sub-G1 increase. Moreover, effects on caspase 3 and PARP cleavage were observed at the highest doses and longest treatment times. We have also determined the effect of enzastaurin *in vivo* in a FL xenograft murine model and shown that even as a single agent this molecule exerts a potent anti-tumour effect. We showed that enzastaurin had a direct effect on RL cells as we observed an induction of apoptosis, as demonstrated by active caspase 3 staining. However, enzastaurin may also have an indirect anti-tumour effect through the inhibition of angiogenesis (supplementary data).

PKC is a key enzyme involved in BCR signalling (Leitges *et al.*, 1996; Guo *et al.*, 2004). Several studies have revealed the role of PKCβ in tumour B-cells such as B-CLL (Abrams *et al.*, 2007), FL and DLBCL (Decouvelaere *et al.*, 2007; Li *et al.*, 2007), where its expression appears to be correlated with lower survival rates. Thus, the PKC inhibitor enzastaurin seemed an interesting drug candidate for FL cells. This drug is a macrocyclic bisindolylmaleimide derivative and an inhibitor of both the PKC and Akt pathways, which are strongly implicated in the amplification of BCR signalling (Guo *et al.*, 2004). Preclinical activity of enzastaurin has been demonstrated in a variety of tumours including B-cell malignancies (Podar *et al.*, 2007b; Chen and LaCasce, 2008; Ysebaert and Morschhauser, 2011). Our study has demonstrated a key role of p90RSK in the effects of enzastaurin on FL cells. This kinase is thought to mediate a number of biological effects and phosphorylates a variety of substrates in different cellular locations. These substrates regulate various biological processes such as transcriptional control, translation, cell-cycle progression, cell proliferation, cell survival and cell motility (Anjum and Blenis, 2008). p90RSK is able to activate mTOR both directly through phosphorylation of raptor (Carrière *et al.* 2008) and indirectly through phosphorylation of TSC2 at Ser^{1789}, in turn inactivating its tumour suppressor functions (Roux *et al.*, 2004). In our study, we did not test whether p90RSK-dependent mTOR inhibition was direct or mediated by TSC2. However, we observed that p90RSK negatively regulated GSK3β by inducing its phosphorylation on Ser^{9}. This can be mediated directly (Sutherland *et al.*, 1993) or indirectly through mTORC1 (Zhang *et al.*, 2006; Carrière *et al.* 2008). Sacchi *et al.* reported that enzastaurin inhibited Akt and mTOR and activated GSK3β in FL cell lines. In contrast with our study, they found that the effects of treatment did not appear until a later time point (Civallero *et al.* 2010).

How enzastaurin targets p90RSK remains to be explored but several hypotheses can be proposed. First, it could be direct as it has been described that PKC inhibitors are able to inactivate p90RSK directly (Roberts *et al.*, 2005). Second, enzastaurin-induced p90RSK inhibition could be the consequence of PKC inhibition as several studies have demonstrated that PKC directly regulates p90RSK (Tan *et al.*, 1999; Bertolotto *et al.*, 2000; Hurbin *et al.*, 2005). However, the discrepancy between the early targeting of p90RSK (6 h) and the late inhibition of PKC phosphorylation (24/48 h; data not shown) by enzastaurin may rule out this hypothesis. Third, enzastaurin could target ERK, which is overactivated in FL cells (Leseux *et al.*, 2008), and would therefore affect p90RSK as this is activated by MAPK (Anjum and Blenis, 2008). Fourth, enzastaurin could inhibit p90RSK through a PDK1 such as Akt (Jensen *et al.*, 1999; Williams *et al.*, 2000). Because PI3K/Akt is overactivated in FL cell lines (Leseux *et al.*, 2006), enzastaurin, which is an Akt inhibitor (Podar *et al.*, 2007), could target p90RSK phosphorylation via this pathway. However, we observed that Akt inhibition by enzastaurin occurred after p90RSK inhibition, so this hypothesis appears unlikely. Finally, it has been proposed that enzastaurin activates phosphatases such as PP2Cγ or PP2A (Dhillon *et al.*, 2002; Doehn *et al.*, 2004; Liffraud *et al.*, 2012). We measured phosphatase activity in FL and did not observe any modifications after enzastaurin treatment (data not shown), excluding a role for PP2A/Cγ in p90RSK inhibition.

Taken together, our study provided *in vitro* and *in vivo* evidence for an anti-lymphoma effect of enzastaurin. We have also provided a better understanding of the signalling mechanisms and their chronological order of action following enzastaurin treatment, and have identified p90RSK as a key target.

Acknowledgements

The authors thank Catherine Trichard for technical assistance, Gaëtan Chicanne for the PI3K assay and Scientific Scripts for proofreading the manuscript. This study was supported by an institutional grant from the INSERM. Samar Kheirallah was the recipient of a grant from l'Association pour la Recherche contre le Cancer.

Authors also acknowledge Imag'IN Platform of the Institut Universitaire du Cancer (https://www.imagin.univ-tlse3.fr/ImagIn/index.php?lang=EN)

Conflict of interest

Karim A. Benhadji is an Eli Lilly employee.

References

Abrams ST, Lakum T, Lin K, Jones GM, Treweeke AT, Farahani M *et al.* (2007). B-cell receptor signaling in chronic lymphocytic leukemia cells is regulated by overexpressed active protein kinase C beta II. Blood 109: 1193–1201.

Alexander DD, Mink PJ, Adami HO, Chang ET, Cole P, Mandel JS *et al.* (2007). The non-Hodgkin lymphomas: a review of the epidemiologic literature. Int J Cancer 120: 1–39.

Anjum R, Blenis J (2008). The RSK family of kinases: emerging roles in cellular signalling. Nat Rev Mol Cell Biol 9: 747–758.

Bertolotto C, Maulon L, Filippa N, Baier G, Auberger P (2000). Protein kinase C theta and epsilon promote T-cell survival by a rsk-dependent phosphorylation and inactivation of BAD. J Biol Chem 275: 37246–37250.

Carrière A, Cargnello M, Julien LA, Gao H, Bonneil E, Thibault P *et al.* (2008). Oncogenic MAPK signaling stimulates mTORC1 activity by promoting RSK-mediated raptor phosphorylation. Curr Biol 18: 1269–1277.

Chen YB, LaCasce AS (2008). Enzastaurin. Expert Opin Investig Drugs 17: 939–944.

Civallero M, Cosenza M, Grisendi G, Marcheselli L, Todoerti K, Sacchi S (2010). Effects of enzastaurin, alone or in combination, on signaling pathway controlling growth and survival of B-cell lymphoma cell lines. Leuk Lymphoma 51: 671–679.

Danial NN (2008). BAD: undertaker by night, candyman by day. Oncogene 27 (Suppl 1): S53–S70.

Decouvelaere AV, Morschhauser F, Buob D, Copin MC, Dumontet C (2007). Heterogeneity of protein kinase C beta(2) expression in lymphoid malignancies. Histopathology 50: 561–566.

Dhillon AS, Meikle S, Yazici Z, Eulitz M, Kolch W (2002). Regulation of Raf-1 activation and signalling by dephosphorylation. EMBO J 21: 64–71.

Doehn U, Gammeltoft S, Shen SH, Jensen CJ (2004). p90 ribosomal S6 kinase 2 is associated with and dephosphorylated by protein phosphatase 2Cdelta. Biochem J 382: 425–431.

Fruchon S, Kheirallah S, Al Saati T, Ysebaert L, Laurent C, Leseux L *et al.* (2012). Involvement of the Syk-mTOR pathway in follicular lymphoma cell invasion and angiogenesis. Leukemia 26: 795–805.

Graff JR, McNulty AM, Hanna KR, Konicek BW, Lynch RL, Bailey SN *et al.* (2005). The protein kinase Cbeta-selective inhibitor, Enzastaurin (LY317615.HCl), suppresses signaling through the AKT pathway, induces apoptosis, and suppresses growth of human colon cancer and glioblastoma xenografts. Cancer Res 65: 7462–7469.

Guertin DA, Sabatini DM (2007). Defining the role of mTOR in cancer. Cancer Cell 12: 9–22.

Gulmann C, Espina V, Petricoin E 3rd, Longo DL, Santi M, Knutsen T *et al.* (2005). Proteomic analysis of apoptotic pathways reveals prognostic factors in follicular lymphoma. Clin Cancer Res 11: 5847–5855.

Guo B, Su TT, Rawlings DJ (2004). Protein kinase C family functions in B-cell activation. Curr Opin Immunol 16: 367–373.

Hans CP, Weisenburger DD, Greiner TC, Chan WC, Aoun P, Cochran GT *et al.* (2005). Expression of PKC-beta or cyclin D2 predicts for inferior survival in diffuse large B-cell lymphoma. Mod Pathol 18: 1377–1384.

Hurbin A, Coll JL, Dubrez-Daloz L, Mari B, Auberger P, Brambilla C *et al.* (2005). Cooperation of amphiregulin and insulin-like growth factor-1 inhibits Bax- and Bad-mediated apoptosis via a protein kinase C-dependent pathway in non-small cell lung cancer cells. J Biol Chem 280: 19757–19767.

Irish JM, Czerwinski DK, Nolan GP, Levy R (2006). Altered B-cell receptor signaling kinetics distinguish human follicular lymphoma B cells from tumor-infiltrating nonmalignant B cells. Blood 108: 3135–3142.

Jensen CJ, Buch MB, Krag TO, Hemmings BA, Gammeltoft S, Frödin M (1999). 90-kDa ribosomal S6 kinase is phosphorylated and activated by 3-phosphoinositide-dependent protein kinase-1. J Biol Chem 274: 27168–27176.

Kilkenny C, Browne W, Cuthill IC, Emerson M, Altman DG (2010). Animal research: Reporting *in vivo* experiments: The ARRIVE guidelines. Br J Pharmacol 160: 1577–1579.

Leitges M, Schmedt C, Guinamard R, Davoust J, Schaal S, Stabel S *et al.* (1996). Immunodeficiency in protein kinase c beta-deficient mice. Science 273: 788–791.

Leseux L, Hamdi SM, Al Saati T, Capilla F, Recher C, Laurent G *et al.* (2006). Syk-dependent mTOR activation in follicular lymphoma cells. Blood 108: 4156–4162.

Leseux L, Laurent G, Laurent C, Rigo M, Blanc A, Olive D *et al.* (2008). PKC zeta mTOR pathway: a new target for rituximab therapy in follicular lymphoma. Blood 111: 285–291.

Li S, Phong M, Lahn M, Brail L, Sutton S, Lin BK *et al.* (2007). Retrospective analysis of protein kinase C-beta (PKC-beta) expression in lymphoid malignancies and its association with survival in diffuse large B-cell lymphomas. Biol Direct 2: 8–20.

Liffraud C, Quillet-Mary A, Fournié JJ, Laurent G, Ysebaert L (2012). Protein phosphatase-2A activation is a critical step for enzastaurin activity in chronic lymphoid leukemia cells. Leuk Lymphoma 53: 966–972.

McGrath J, Drummond G, McLachlan E, Kilkenny C, Wainwright C (2010). Guidelines for reporting experiments involving animals: the ARRIVE guidelines. Br J Pharmacol 160: 1573–1576.

Moreau AS, Jia X, Ngo HT, Leleu X, O'Sullivan G, Alsayed Y *et al.* (2007). Protein kinase C inhibitor enzastaurin induces *in vitro* and *in vivo* antitumor activity in Waldenstrom macroglobulinemia. Blood 109: 4964–4972.

Podar K, Raab MS, Zhang J, McMillin D, Breitkreutz I, Tai YT *et al.* (2007a). Targeting PKC in multiple myeloma: *in vitro* and *in vivo* effects of the novel, orally available small-molecule inhibitor enzastaurin (LY317615.HCl). Blood 109: 1669–1677.

Podar K, Raab MS, Chauhan D, Anderson KC (2007b). The therapeutic role of targeting protein kinase C in solid and hematologic malignancies. Expert Opin Investig Drugs 16: 1693–1707.

Roberts NA, Haworth RS, Avkiran M (2005). Effects of bisindolylmaleimide PKC inhibitors on p90RSK activity *in vitro* and in adult ventricular myocytes. Br J Pharmacol 145: 477–489.

Roux PP, Ballif BA, Anjum R, Gygi SP, Blenis J (2004). Tumor-promoting phorbol esters and activated Ras inactivate the tuberous sclerosis tumor suppressor complex via p90 ribosomal S6 kinase. Proc Natl Acad Sci U S A 101: 13489–13494.

Shipp MA, Ross KN, Tamayo P, Weng AP, Kutok JL, Aguiar RC *et al*. (2002). Diffuse large B-cell lymphoma outcome prediction by gene-expression profiling and supervised machine learning. Nat Med 8: 68–74.

Sutherland C, Leighton IA, Cohen P (1993). Inactivation of glycogen synthase kinase-3 beta by phosphorylation: new kinase connections in insulin and growth-factor signalling. Biochem J 296: 15–19.

Tan Y, Ruan H, Demeter MR, Comb MJ (1999). p90(RSK) blocks bad-mediated cell death via a protein kinase C-dependent pathway. J Biol Chem 274: 34859–34867.

Williams MR, Arthur JS, Balendran A, van der Kaay J, Poli V, Cohen P *et al*. (2000). The role of 3-phosphoinositide-dependent protein kinase 1 in activating AGC kinases defined in embryonic stem cells. Curr Biol 10: 439–448.

Ysebaert L, Morschhauser F (2011). Enzastaurin hydrochloride for lymphoma: reassessing the results of clinical trials in light of recent advances in the biology of B-cell malignancies. Expert Opin Investig Drugs 20: 1167–1174.

Zha H, Raffeld M, Charboneau L, Pittaluga S, Kwak LW, Petricoin E *et al*. (2004). Similarities of prosurvival signals in Bcl-2-positive and Bcl-2-negative follicular lymphomas identified by reverse phase protein microarray. Lab Invest 84: 235–244.

Zhang HH, Lipovsky AI, Dibble CC, Sahin M, Manning BD (2006). S6K1 regulates GSK3 under conditions of mTOR-dependent feedback inhibition of Akt. Mol Cell 24: 185–197.

Supporting information

Additional Supporting Information may be found in the online version of this article at the publisher's web-site:

http://dx.doi.org/10.1111/bph.12351

Figure S1 Inhibition of secreted VEGF by enzastaurin in FL cells. RL and DOHH2 cells were treated with 5 μM of enzastaurin or with vehicle (DMSO). Secreted VEGF in the cell supernatant was measured at 72 h. Histograms are expressed in pg mL^{-1} and are the mean of three independent experiments ± SD. *$P < 0.01$.